

Obtaining the Radiated Gravitational Wave Energy via Relativistic Kinetic Theory: A Kinetic Gas Model of an Idealized Coalescing Binary

Noah M. MacKay ^a

^a*Universität Potsdam, Institute of Physics and Astronomy, Karl-Liebknecht-Straße
24/25, 14476, Potsdam, Germany*

Abstract

The final pulse of gravitational wave emission is released in the chirp phase of binary coalescence. This proposes that the radiated energy of the GW is proportional to the chirp mass \mathcal{M} , with detection reports revealing the approximate scaling of $E_{\text{GW}} \approx \mathcal{M}/10$. While this scaling is evident in numerical relativity, there lacks an analytical expression supporting the relation. This study utilizes a heuristic application of relativistic kinetic theory and massless Bose-Einstein statistics for an entropic graviton gas to GW formation throughout binary coalescence. This approach to GW formation obtains an expression of an effective thermal energy as the radiated GW energy, which extracts the nearly one-tenth scaling of the chirp mass, namely at the chirp phase. Furthermore, it agrees well with the detected energies with 1:1 ratio values ranging from 0.932 for GW150914 to 0.998 for one of three waveform models of GW190521, with 0.851 as an outlier for GW170104. Establishing a quantum-classical correspondence in this regard enables discussion of equilibrium noise analysis on the graviton gas as well as its kinetic characteristics during and after coalescence. The latter topic includes, but is not limited to, GW/graviton wave-particle duality, a calculation of the high-energy graviton-graviton total cross section as 1.16% of the chirp mass surface area $A = 16\pi G^2 \mathcal{M}^2$, and humoring the thought experiment of black hole gravitons.

Keywords: Gravitational Waves, Relativistic Kinetic Theory, Graviton Gas, GW Astronomy and Phenomenology

1. Introduction

On 14 September 2015, laser interferometer detectors at LIGO read a signal from a gravitational wave (GW) formed by a coalescing black hole binary [1]. Characteristics of the source black hole binary that released GW150914 were determined by Bayesian analysis: the initial total mass was $M \simeq (29 + 35)M_\odot$, calculating a chirp mass $\mathcal{M} = \alpha^{3/5}M$ to be $\sim 28M_\odot$, and the final remnant mass was $m_f \simeq 62M_\odot$. Here, $\alpha = m_1m_2/M^2$ is the so-called symmetric mass ratio, and $M_\odot \simeq 2 \times 10^{30}$ kg defines the solar mass. With the remainder of the initial total mass from the final mass converted into the emitted, i.e., radiated energy of the GW, this leaves with $E_{\text{GW}} \simeq 2M_\odot$ with $c = 1$. At first glance, this shows that E_{GW} roughly approximates to a tenth of the chirp mass, as the final pulse of GW formation is sent out at the chirp phase of coalescence. This trend continues into further GW detections, regardless of coalescing binary type [2, 3, 4, 5, 6, 7]¹. Although $E_{\text{GW}} \approx \mathcal{M}/10$ is evident in the numerics of numerical relativity, there is yet an analytical expression to show this proportionality.

While the quantum theory of gravity is an ongoing endeavor, the detection of GW150914 and following GWs reinvigorated the notion of classical-quantum correspondence (QCC) between the GW and the bosonic graviton [3, 8, 9, 10, 11]. In these reports, gravitons are perceived to be the particle counterpart to GWs and the quantum noise in the GW background; as bosons they follow Bose-Einstein (BE) statistics. Should one make the connection between GW formation and a system of “noisy” gravitons, a framework is needed in such a way that statistical mechanics and relativistic kinetic theory (RK-Theory) can reinterpret the astrophysics of GW formation.

A consequence of applying RK-Theory to GW formation is the treatment of the noisy gravitons as an ultra-relativistic ideal gas. The entropy of this ideal gas is not induced by the temperature of the system-background ensemble with $T \sim 1\text{K}$ [9, 10], but rather by the excitations from macroscopic gravitational attraction as well as high-energy graviton-graviton scatterings [12, 13, 14, 15, 16]. As the binary coalesces from the inspiral to chirp phases, the ideal graviton gas is enclosed within a spherical volume whose equatorial plane is traced by the binary masses (assuming no angular projection of the xy-plane, i.e., $\mathcal{R}[\iota] = \mathbb{1}$). Throughout coalescence, this surface exhibits

¹This is a selection of all observation papers from LIGO up to the current O4 observation run, which importantly list E_{GW} and \mathcal{M} .

the characteristics of an extreme Kerr outer surface: relativistic equatorial rotations with a contracting radius. As a result, the chirp phase relates to the presence of the chirp mass \mathcal{M} (i.e., the surface area is in terms of its Schwarzschild radius $r_S = 2G\mathcal{M}$) and the final pulse in GW emission having the energy $E_{\text{GW}} \propto \mathcal{M}$.

The parameter that can connect GW astrophysics with RK-Theory is the energy density ϵ , which is the first diagonal entry of the energy-stress (also called energy-momentum) tensor $T_{\mu\nu}$. For the cases of general relativity (GR) and RK-Theory, the tensor is respectively defined in terms of geometric curvature and as a Lorentz-invariant momentum-space integral. Specifically, $T_{00} \equiv \epsilon$ defines the amount of energy contained in the coalescing binary volume. Assuming there is an effective thermal equilibrium, this internal energy at the chirp phase is the emitted GW energy outside the surface. The provided study investigates the notion of QCC via the energy density, whether the relation between a rotating body and RK-Theory under massless BE statistics extracts the dissipated energy as the analytical GW energy at the chirp phase (i.e., whether the RK-Theory of a graviton gas mirrors the astrophysics of GW formation). An idealized visual aid of the kinetic gas model of a coalescing binary is provided in Figure 1 as a computationally simulated image.

2. Methods

2.1. Contracting Surface Model

As stable binary systems can be treated as a singular system by utilizing the reduced mass $\mu = m_1 m_2 / M$, we can approach a coalescing binary the same way, however using a time-dependent “enclosed mass” function $M_{\text{encl}}(t)$. Adding time dependence to the enclosed mass allows the consideration of the total mass M for times $t < t_C$, where t_C is the coalescence time, the chirp mass \mathcal{M} at the singular time $t = t_C$, and the final remnant mass m_f for times $t > t_C$.

In addition to the enclosed mass as a function of time, the surface traced by the coalescing binary would be idealized as an intensifying Kerr surface with accelerated rotations and a contracting radius $r = r(t)$. In the respective timelapse as the enclosed mass, the diameter $d(t < t_C) \equiv 2r(t < t_C)$ encloses the instantaneous separation distance and the two masses before coalescence; $r(t = t_C) = 2G\mathcal{M}$ at the chirp phase, and finally $r(t > t_C)$ is the radius of

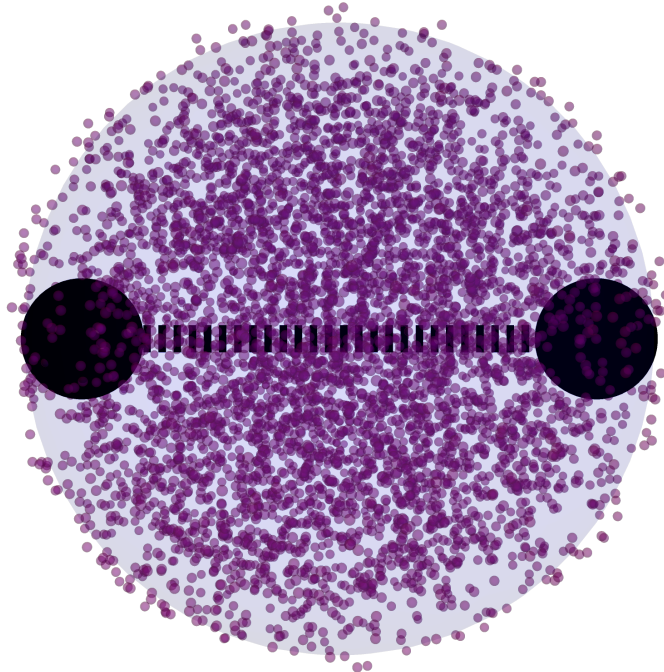


Figure 1: An idealized visual aid of the kinetic gas model of a coalescing binary. The binary masses (black spheres), whose separation distance is drawn by the dashed black line, are enclosed in a larger volume (lavender sphere) representing a rotating body. Contained within and along the rotating surface is an ideal graviton gas (sea of purple particles); particles outside resemble intermediate GWs throughout coalescence. As the separation distance decreases, the volume contracts; the enclosed energy density of the gas is set to be equal to the energy density along the rotating surface.

the remnant mass after coalescence. Determining $r(t \leq t_C)$ as an expression is offered in Appendix A.

The energy-stress tensor $T_{\mu\nu}$ stands on the right-hand side of the Einstein Field Equations (EFEs): $G_{\mu\nu} = 8\pi G T_{\mu\nu}$. Here, $G_{\mu\nu}$ is the Einstein tensor that is constructed by the metric and Ricci curvature tensors as $R_{\mu\nu} - Rg_{\mu\nu}/2$; the additive cosmological contribution $\Lambda g_{\mu\nu}$ is neglected. In addition, the metric tensor $g_{\mu\nu}$ is typically linearized to consider a canonical Minkowski metric and a small perturbation that indicates the presence of GWs: $\eta_{\mu\nu} + h_{\mu\nu}$ respectively.

As our model of a coalescing binary resembles a rotating body with mass

$M_{\text{encl}}(t)$ and radius $r(t)$, defining $T_{\mu\nu}$ from the EFEs is straight-forward:

$$T_{\mu\nu} = \frac{1}{8\pi G} G_{\mu\nu}; \quad (1)$$

its energy density $\epsilon \equiv T_{00}$ is defined as follows (c.f. Ref. [17]):

$$T_{00} = \frac{-1}{8\pi G} \left(\vec{\Gamma}^2 + \vec{\Omega}^2 \right) = \frac{-GM_{\text{encl}}(t)^2}{8\pi r(t)^4} \left(1 + \frac{\beta^2}{4} \right), \quad (2)$$

which is negative in value. Here, $\vec{\Gamma}$ is the gravitational field strength and $\vec{\Omega}$ is the gravitational torsion field, generally defined with a radial variable $r \in [0, \infty)$; both fields are specially defined for the coalescing surface at the given radius $r(t)$. From the torsion field, $\beta = |\vec{v}|/c$ in SI units, where \vec{v} is the tangential velocity of rotation. For a coalescing binary, \vec{v} is the accelerating orbital velocity.

Thus, given Eq. (2), the ratio β is also expected to change throughout coalescence, i.e., approach unity leading to coalescence. Having $\beta = 1$ at $t = t_C$ is to denote extremely relativistic rotations of the coalescing binary, where correspondingly $M_{\text{encl}}(t_C) = \mathcal{M}$ and $r(t_C) = 2G\mathcal{M}$. Appendix B.1 offers a more straight-forward derivation of radiated energy from a rotating body under the chirp phase conditions, ignoring RK-Theory altogether. This is accompanied by 1:1 ratio values between the classical answers and the detected values.

2.2. RK-Theory

In relativistic kinetic theory, the energy-momentum tensor is generally defined as a Lorentz-invariant momentum-space integral in the following form [18]:

$$T^{\mu\nu} = \sum_a \int_{-\infty}^{\infty} \frac{d^3\vec{p}_a}{(2\pi\hbar)^3} \frac{p_a^\mu p_a^\nu}{E_a} f(\vec{p}_a), \quad (3)$$

where \hbar is the reduced Planck constant; the quantity $(2\pi\hbar)^3$ defines a phase space volume. Also, $p_a^\mu = (E_a, \vec{p}_a)$ is the 4-momentum vector of a particle of species type a , with $E_a = \sqrt{|\vec{p}_a|^2 + m_a^2}$ being its energy, and $f(\vec{p}_a)$ is a distribution function of the particles of species a within a defined enclosure. As we are implying an ideal and ultra-relativistic graviton gas, the summation drops as we are dealing with a pure (i.e., one-component) gas, and the distribution function is the massless Bose-Einstein distribution with quantum

degrees of freedom d_j :

$$f(\vec{p}) = \frac{d_j}{\exp(|\vec{p}|/\Theta) - 1}. \quad (4)$$

In the above, $d_j = 2$ for massless gravitons². While gravitons are spin-2 bosons due to the energy-momentum tensor being the source of gravity in GR [13], the degrees of freedom reflect the traceless and transverse (TT) gauges of GW polarization (i.e., $\eta^{\mu\nu}h_{\mu\nu}^{\text{TT}} = 0$ and $p^\mu h_{\mu\nu}^{\text{TT}} = 0$), which is analogous to the Lorentz and Coulomb gauges for photons.

In a thermodynamic context, Θ in Eq. (4) typically denotes the thermal energy of the gas within a closed system. However, in the given context of GW formation, Θ instead defines an *effective* thermal energy (i.e., an entropic energy) for the noisy gravitons in the coalescing system. This relates to the expected energy of an emitted GW, assuming there is an effective thermal equilibrium within the system-background ensemble. Therefore, Θ is the quantity we aim to define.

Via Eq. (3), the energy density is defined as an integral (which is positive in value, and with no mass for the gravitons):

$$T^{00} \equiv \epsilon = \int_{-\infty}^{\infty} \frac{d^3\vec{p}}{(2\pi\hbar)^3} |\vec{p}| f(\vec{p}) \quad (5)$$

(note that $T^{00} := T_{00}$), with $E = |\vec{p}|$ for massless particles and the distribution function acknowledged to be Eq. (4). From statistical mechanics, the definitions for the number density $n \equiv N/V$ and the average of a quantity q under any distribution are defined as

$$\begin{aligned} n &= \int_{-\infty}^{\infty} \frac{d^3\vec{p}}{(2\pi\hbar)^3} f_0(\vec{p}), & \langle q \rangle &= \frac{1}{Z_0} \int_{-\infty}^{\infty} d^3\vec{p} q(\vec{p}) f_0(\vec{p}), \\ Z_0 &\equiv \int_{-\infty}^{\infty} d^3\vec{p} f_0(\vec{p}) = n(2\pi\hbar)^3. \end{aligned} \quad (6)$$

From these definitions, the massless BE energy density is straight-forwardly

$$T^{00} \equiv n\langle E \rangle = \frac{\bar{N}_{\text{BE}}}{V} \frac{\pi^4}{30\zeta(3)} \Theta. \quad (7)$$

²For hypothetical massive gravitons, $d_j \equiv 2s + 1 = 5$ due to the helicities $(\pm 2, \pm 1, 0)$.

In Eq. (7), \bar{N}_{BE} is the spin-averaged number of BE-distributed particles in one microstate. Provided that the microstatic energy $\varepsilon > \Theta$, all bosons occupy one microstate. Allowing the graviton's microstatic energy be generally $\varepsilon = \hbar\omega$, the spin-averaged microstate number is expressed in the form of the Planck distribution:

$$\bar{N}_{\text{BE}} = \frac{1}{\exp(\hbar\omega/\Theta) - 1}. \quad (8)$$

For asymptotically large entropic energy Θ , which is to be expected for RK-Theory to mirror GW astrophysics, the coupling of $\bar{N}_{\text{BE}}\Theta$ takes on the approximate form:

$$\lim_{\Theta \rightarrow \infty} \bar{N}_{\text{BE}}\Theta \simeq \frac{\Theta^2}{\hbar\omega}. \quad (9)$$

Also in Eq. (7), V is the volume of the system, i.e., the coalescing body where $V(t) \propto r(t)^3$, and $\zeta(a)$ is the Riemann zeta function of argument a :

$$\zeta(a) = \frac{1}{(a-1)!} \int_0^\infty \frac{x^{a-1}}{e^x - 1} dx. \quad (10)$$

Appendix B.2 discusses an alternative, semi-classical derivation of the total energy ϵV by overlooking the entropic energy, and by considering $\langle E \rangle = M_{\text{encl}}(t)$ to illustrate that the expected energy enclosed is the rest energy of the macroscopic enclosed mass. A condition is to leave the microstatic number unaveraged by graviton spin, and that the resulting equation is valid for only one phase of binary coalescence: the chirp phase.

3. E_{GW} as Entropic Energy

Inserting the asymptotic approximation expressed as Eq. (9) in its place in Eq. (7), the expression is set to be approximate to Eq. (2); considering that the volume of the coalescing surface is spherical, we have

$$\frac{-GM_{\text{encl}}(t)^2}{r(t)} \left(1 + \frac{\beta(t)^2}{4} \right) \simeq \frac{\pi^4}{5\zeta(3)} \frac{\Theta^2}{\hbar\omega}. \quad (11)$$

The frequency associated with microstatic energy ω relates inversely to the mean free path: the average distance traveled between consecutive collisions with nearest neighbors, i.e., $\omega \propto \lambda^{-1}$. Given the statistical number density with unspecified volume (i.e., given the definition of n in Eq. [6]),

the free mean path also depends on the scattering cross section obtained via quantum field theory: $\lambda \propto (n\sigma)^{-1}$. In the provided case of QCC for GW formation, the free mean path within a specified volume $V \propto r(t)^3$ is an average spacing between particles. As the volume is contracting throughout coalescence, the microstatic energy increases to reflect the increased interactions within a tighter space. Characteristically, the thermal de Broglie wavelength can be used as the mean free path:

$$\lambda_{\text{th}} = \frac{\pi^{2/3}\hbar}{\Theta}, \quad (12)$$

from which a thermal frequency can be defined as $\omega_{\text{th}} = 2\pi/\lambda_{\text{th}}$. Thus, with $\varepsilon = 2\pi^{1/3}\Theta > \Theta$, all gravitons are in one microstate. We have

$$\frac{-GM_{\text{encl}}(t)^2}{r(t)} \left(1 + \frac{\beta(t)^2}{4}\right) \simeq 5.5330\Theta, \quad (13)$$

which solves for the entropic energy Θ at any time throughout coalescence as

$$\Theta(t) \simeq -0.18074 \frac{GM_{\text{encl}}(t)^2}{r(t)} \left(1 + \frac{\beta(t)^2}{4}\right). \quad (14)$$

Essentially, given Eq. (14), the emitted GW energy throughout coalescence is obtainable, provided that we have full knowledge of the parameters $M_{\text{encl}}(t)$, $r(t)$, and $\beta(t)$ within the coalescence timelapse. Specifically at the chirp phase, i.e., at time $t = t_C$, our parameters are $M_{\text{encl}}(t_C) = \mathcal{M}$, $r(t_C) = 2G\mathcal{M}$, and $\beta(t_C) = 1$:

$$\Theta(t_C) \equiv \Theta_{\text{chirp}} \simeq -0.11296 \mathcal{M}, \quad (15)$$

which obtains the $\mathcal{M}/10$ proportionality for the GW energy emitted at the chirp phase. Figure 2 provides two illustrations of the idealized kinetic gas model initially shown in Figure 1 undergoing coalescence. Binary collapse is demonstrated from left to right, during which the increase of microstatic energy via increased particle interactions is induced.

Table 1 offers select GWs detected by LIGO, where the chirp mass \mathcal{M} and the emitted GW energy E_{GW} are either well known or obtainable. These discoveries were documented in Refs. [1, 2, 3, 4, 5, 6, 7]³. Also in the table,

³For the detection of GW190521, three waveform models were used in Ref. [7] to extract parameters, such as \mathcal{M} ; the emitted energy $E_{\text{GW}} = M - m_f$ and $|\Theta_{\text{chirp}}| \propto \mathcal{M}$ are calculated in Table 1 for all models, avoid of statistical errors.

the magnitudes of Θ_{chirp} are calculated and compared with the emitted GW energy. As provided in the table, $|\Theta_{\text{chirp}}|$ calculates values of energy that are within the statistical errors of the true values of E_{GW} . One can claim that the observed quantities and the expected values agree well via the corresponding 1:1 ratios.

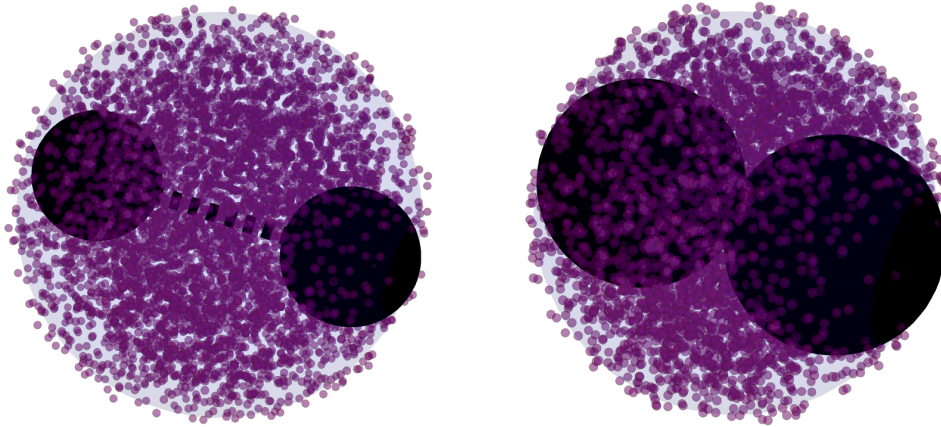


Figure 2: From left to right, a progression towards coalescence of the kinetic gas model. The encroachment of the binary masses (black spheres) and decrease in separation distance contracts the diameter of the coalescing surface (lavender sphere). The graviton gas (sea of purple particles) becomes more compact as a result, illustrating an increase in graviton-graviton interactions and in the energy density.

4. Discussion

To reiterate, the question proposed in Section 1 was whether the radiated energy of a gravitational wave can be analytically expressed as a mirroring between the relativistic kinetic theory of a graviton gas and the astrophysics of gravitational wave formation. After discussions of the methods used to build a framework between a contracting rotating body and kinetic theory, the equation of energy densities between Eqs. (2) and (7) led to a relation of radiated energy that illustrates the roughly one-tenth scaling of the chirp mass, a characteristic that is well understood in numerical relativity.

This demonstrates that, via the derivation of Eq. (15), the analytical expression of what is evident in numerical relativity comes from an inherent QCC between GW formation and the kinetic theory of a graviton gas. While

GW Name	\mathcal{M}	E_{GW} (SI Units)	$ \Theta_{\text{chirp}} $ (SI Units)	1:1 Ratio
GW150914	$28.1^{+3.9}_{-3.5}M_{\odot}$	$3.0^{+0.5}_{-0.5}M_{\odot}c^2$	$3.22M_{\odot}c^2$	0.9317
GW151226	$8.9^{+0.3}_{-0.3}M_{\odot}$	$1.0^{+0.1}_{-0.2}M_{\odot}c^2$	$1.01M_{\odot}c^2$	0.9901
GW170104	$21.1^{+2.4}_{-2.7}M_{\odot}$	$2.0^{+0.6}_{-0.7}M_{\odot}c^2$	$2.35M_{\odot}c^2$	0.8511
GW170608	$7.9^{+0.2}_{-0.2}M_{\odot}$	$0.85^{+0.07}_{-0.17}M_{\odot}c^2$	$0.89M_{\odot}c^2$	0.9551
GW170814	$24.1^{+1.4}_{-1.4}M_{\odot}$	$2.7^{+0.4}_{-0.3}M_{\odot}c^2$	$2.72M_{\odot}c^2$	0.9927
GW190521	$64.0^{+13}_{-8}M_{\odot}$	$8.0M_{\odot}c^2$	$7.23M_{\odot}c^2$	0.9038
	$65.0^{+11}_{-7}M_{\odot}$	$7.0M_{\odot}c^2$	$7.34M_{\odot}c^2$	0.9537
	$71.0^{+15}_{-10}M_{\odot}$	$8.0M_{\odot}c^2$	$8.02M_{\odot}c^2$	0.9975

Table 1: Emitted energies and associated chirp masses of select GWs detected by LIGO. The effective thermal energies at the chirp phase (Eq. [15]) are calculated for each corresponding chirp mass for comparison with E_{GW} with a 1:1 ratio.

this “quantization” of GW formation was based on noisy gravitons rather than conventional QFT procedures and string phenomenology, this may arguably strengthen the proposition of gravitons being the quantum noise of macroscopic GWs. This enables open-ended discussion on graviton kinematics and how it contributes to this entropic direction of GW formation.

4.1. The Einstein-Langevin Equation

Treating the gravitons within the coalescing surface as a Brownian bath, another statistical application to GW formation lies in the direction of noise analysis. The Einstein-Langevin (EL) equation was derived in Ref. [19], rewriting the EFEs as a Langevin-like equation describing the stochastic jitters of Brownian motion. In this derivation, the motivation is to connect quantum noise with classical fluctuations, i.e., the gravitons to small metric perturbations of first order h . The resulting integro-differential equation is defined for an enclosed volume V containing fluctuating gravitons; the background of this volume is a flat spacetime. It is written in terms of the

cosmological constant Λ , and the equation uses the Friedmann-Robertson-Walker variables:

$$\ddot{a} - \frac{2}{3}\Lambda a^3 + \frac{\hbar G}{12\pi a} \int_{\tau_i}^{\tau} d\tau' \frac{\dot{a}(\tau')}{a(\tau')} \int_0^{\infty} dk k^3 \cos[k(\tau - \tau')] = \frac{4\pi G}{3Va} \dot{\vartheta}_2(\tau). \quad (16)$$

Here, $a = a(\tau)$ with $\tau = \int dt/a$ being the conformal time; every time derivative present (denoted as the dot notation $\dot{\square}$) is a derivative with respect to τ .

The integrals on the left hand side define a kernel for the quanta dissipation force. On the right hand side, the Gaussian noise generator $\vartheta_2(\tau)$ is subjugated to a conformal time derivative. Ignoring the cosmological constant, i.e., with $\Lambda = 0$, we reduce the order of the EL equation by evaluating both sides over $d\tau$:

$$\dot{a} + \frac{\hbar G}{12\pi} \int \frac{d\tau}{a(\tau)} \int_{\tau_i}^{\tau} d\tau' \frac{\dot{a}(\tau')}{a(\tau')} \int_0^{\infty} dk k^3 \cos[k(\tau - \tau')] = \frac{4\pi G}{3Va} \vartheta_2(\tau); \quad (17)$$

this looks more closely to the standard Langevin equation of the generalized form [20]:

$$\frac{d}{dt} \vec{x}(t) + \vec{\nabla} U(\vec{x}) = \sigma \vartheta_2(t). \quad (18)$$

Here, $U(\vec{x})$ is the potential energy profile of the Brownian bath; its negative gradient calculates the noise dissipation force $\vec{F}(\vec{x}) = -\vec{\nabla} U(\vec{x})$. Also, σ is a proportionality coefficient between stochastic force and noise generation.

Simplifying the 3-integral kernel in Eq. (17), so that the EL equation is expressed as amiable as Eq. (18), is beyond the scope of this discussion. However, once that objective is completed, the quantum noise produced by the graviton gas within the volume V can be numerically iterated. Numerical iteration demands the discretization of the Langevin(-like) equation into an Euler scheme [21], such that (for Eq. [18])

$$x_{i+1} = x_i + \left[F(x_i) + \sigma \frac{\theta_{i,2}}{\sqrt{\Delta t}} \right] \Delta t, \quad (19)$$

where $\theta_{i,2}$ is the i -th random number from a Gaussian distribution within a sequence of jitters. In practice, one sets the range of the index i as $i \in [1, l]$, where l is the maximum number of jitters a sample particle undergoes. Other input parameters for this scheme are $x_1 \simeq 10^{-4}$ (to quantify the natural resting point without inducing calculational infinities) and Δt .

Eq. (19) could become inaccurate with an exceedingly large dissipation force $F(x_i)$ compared to the noise generator; this can be rectified by letting Δt be small, which in turn would make $\Delta x_i = x_{i+1} - x_i$ just as small. The smallness of Δx_i would consider the discreteness of the iterations as continuous; thus, we look at Eq. (18) again. To implement Eq. (19) in the *Mathematica* computation software, for instance, the commands “Random-Variate” and “StableDistribution” and a few lines of code readily generate a large set of Gaussian-distributed numbers, thereby simulating Eq. (18) as a noise signal [21].

4.2. Graviton Gas At Coalescence

4.2.1. Ejected Gravitons as a GW Packet

A wave-particle duality between chirp-phase GWs and a packet of gravitons supposes that the analytical emitted energy (provided as the absolute value of Eq. [15]) relates to the Planck-Einstein energy of N monochromatic gravitons, i.e., $N \times 2\pi\hbar f_{\text{GW}}$. Here, f_{GW} is the frequency of the GW upon detection, which is expected to be the frequency at the chirp phase provided no wave-dampening. Treating the gravitons as though they are photon-like in that regard, the number of gravitons in any emitted GW depends on astrophysical parameters:

$$N_{\text{GW/grav}} \simeq 0.01798 \frac{\mathcal{M}}{\hbar f_{\text{GW}}}. \quad (20)$$

As provided in Eq. (20), the direct proportionality with graviton number and chirp mass relates to the direct scaling of the chirp mass with emitted energy. Likewise, the inverse proportionality with the number and the GW frequency relates to the energy-time uncertainty principle; the higher the frequency, the lower the number due to “uncertainty cloaking”.

E.g., for GW150914 with a source chirp mass of $\mathcal{M} \sim 28M_{\odot}$ and a frequency of $f_{\text{GW}} \sim 200$ Hz [1], the number of gravitons approximates to be 4.531×10^{78} . For GW170104 with a source chirp mass of $\mathcal{M} \sim 21M_{\odot}$ and a frequency of $f_{\text{GW}} \sim 20$ Hz [3], the graviton number approximates to 3.398×10^{79} .

4.2.2. Graviton-Graviton Total Cross Section

In a graviton gas, graviton-graviton scatterings are inevitable. While a quantum theory of gravity is an ongoing endeavor, Feynman rules are applied to an effective field theory of gravity [13], whereby the square of the gauge

coupling for quantum geometro-dynamic (QGD) diagrams is proportional to the EFE coefficient: $g^2 = 8\pi G/\hbar$. Other literature express the gauge coupling squared as inversely proportional to the square of the Planck mass $m_P \equiv \sqrt{\hbar/G} = 2.176 \times 10^{-8}$ kg, such that $g^2 = 8\pi/m_P^2$ [15, 16].

At tree level [13, 15, 16], the total amplitude of the graviton-graviton interaction in QGD accounts for different exchange channels and the ± 2 up/down helicity permutations for the incoming and outgoing gravitons:

$$\mathcal{A}_{\text{tot}} = g^2 \left(\frac{\hat{s}^3}{\hat{t}\hat{u}} + \frac{\hat{u}^3}{\hat{s}\hat{t}} + \frac{\hat{t}^3}{\hat{s}\hat{u}} \right). \quad (21)$$

In the above, \hat{s} , \hat{t} , \hat{u} are the standard Mandelstam variables for Feynman diagram calculations ($\sqrt{\hat{s}}$ relates to center of momentum energy; both $\sqrt{\hat{t}}$ and $\sqrt{\hat{u}}$ relate to momentum transfer). For massless particles, such as gravitons, $\hat{u} = -\hat{t} - \hat{s}$, which implies that Eq. (21) purely depends on the \hat{s} - and \hat{t} -Mandelstam variables.

Given Eq. (21), graviton-graviton scatterings exhibit infrared divergence at the low-energy regime. This is due to the $\hat{t}^3/(\hat{s}\hat{u})$ channel for small \hat{s} , with $\hat{u} = -\hat{t} - \hat{s}$ implied [16]. However, for GW formation, the gravitons are highly entropic, therefore subjugated in the high-energy regime. Eq. (21) is revised accordingly for asymptotically large \hat{s} and factored by 1/2 to correct the over-counting of identical exchange channels for same-species particles [15]:

$$\lim_{\hat{s} \rightarrow \infty} \mathcal{A}_{\text{tot}} \equiv \mathcal{A}_{\text{he}} = -\frac{8\pi G}{\hbar} \frac{\hat{s}^2}{\hat{t}}. \quad (22)$$

Differential cross sections are proportional to the average-magnitude-square of the total amplitude: $d\sigma/d\hat{t} \propto \langle |\mathcal{A}_{\text{tot}}|^2 \rangle$ [22]. For Eq. (22), the square of its magnitude is averaged by the spin factors of the incoming gravitons: $2^2 = 4$. Therefore,

$$\langle |\mathcal{A}_{\text{he}}|^2 \rangle = \frac{16\pi^2 G^2}{\hbar^2} \frac{\hat{s}^4}{\hat{t}^2}, \quad (23)$$

which obtains the resulting differential cross section, and total cross section, as

$$\frac{d\sigma}{d\hat{t}} \equiv \frac{\hbar^2}{16\pi\hat{s}^2} \langle |\mathcal{A}_{\text{he}}|^2 \rangle = \pi G^2 \frac{\hat{s}^2}{\hat{t}^2}, \quad \sigma_{\text{he}} \simeq \int_{-\hat{s}}^{\hat{s}} \frac{d\sigma}{d\hat{t}} d\hat{t} = \pi G^2 \hat{s}. \quad (24)$$

Since the total cross section is energy-dependent, i.e., dependent on \hat{s} , the so-called thermal average of the cross section is to be evaluate to remove

energy dependence and extract an average value based on (effective) thermal energy. This thermal average depends on the statistics of the two interacting particles contributing to the cross section calculation. For graviton-graviton scatterings, this thermal average depends on the BE statistics of the two interacting gravitons:

$$\langle\sigma_{\text{he}}\rangle = \pi G^2 \langle\hat{s}\rangle = 14.5927\pi G^2 \Theta^2 \quad (25)$$

(The derivation of $\langle\hat{s}\rangle$ under BE statistics is offered in Appendix C). Therefore, the average cross section of graviton-graviton scatterings throughout coalescence depends on the entropic energy via Eq. (14). At the chirp phase,

$$\langle\sigma_{\text{he}}\rangle = 0.1862\pi G^2 \mathcal{M}^2, \quad (26)$$

which is 1.16% of the chirp mass surface area $A = 16\pi G^2 \mathcal{M}^2$.

4.2.3. λ_{th} at the Chirp Phase

An essential parameter contributing to the derivation of Eq. (15) is the thermal de Broglie wavelength: $\lambda_{\text{th}} = \pi^{2/3} \hbar / \Theta$. This measurement of length relates to the spacing between particles (such as the gravitons) in a gas. Throughout coalescence, $\lambda_{\text{th}} \propto 1/|\Theta(t)|$ via Eq. (14); at the chirp phase, the wavelength is dependent on one astrophysical parameter: the chirp mass:

$$\lambda_{\text{th, chirp}} = 18.9893 \frac{\hbar}{\mathcal{M}}. \quad (27)$$

In the above, the chirp phase thermal wavelength takes the form similar to the reduced Compton wavelength of the chirp mass. E.g., for GW150914 with a source chirp mass of $\mathcal{M} \sim 28M_{\odot}$ [1], the thermal wavelength has a value of 1.1303×10^{-73} m. For GW170104 with a source chirp mass of $\mathcal{M} \sim 21M_{\odot}$ [3], the wavelength has a value of 1.5071×10^{-73} m. These values of length are significantly smaller than the Planck length: $l_P \equiv \sqrt{\hbar G} = 1.616 \times 10^{-35}$ m, which can be in itself a discussion topic in the context of Planck-scale physics, such as loop quantum gravity (LQG) and the “spin-foam” lattice structure of spacetime [23, 24, 25].

In the Planck scale, where l_P is itself a unit of measurement, the sample values of $\lambda_{\text{th, chirp}}$ have the order of magnitude of $\sim 10^{-38} l_P$. That is, given that astronomical masses of the binary are the source of entropy for the graviton gas; graviton entropy in canonically flat spacetime might be a possible topic of research. This leads to a consequential event of a graviton gas

after coalescence, i.e., a graviton gas trapped in the remnant mass. Figure 3 illustrates the merger of the binary masses to become the remnant mass, with ejected gravitons outside the merger and remaining gravitons trapped within the remnant surface.

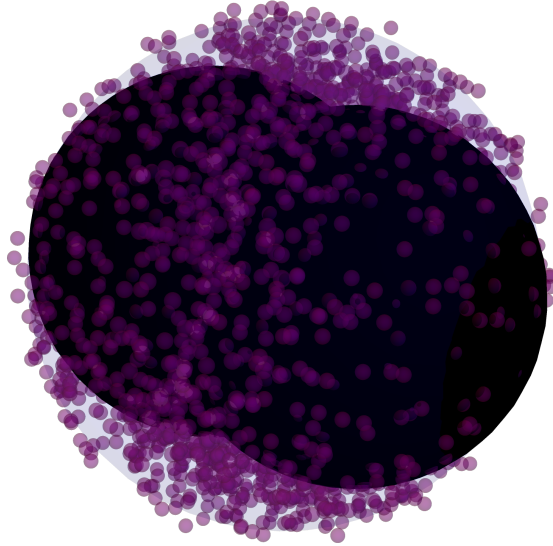


Figure 3: The coalescing binary approximately at the chirp phase. The binary masses (black spheres) are merging into one remnant mass, with the larger volume (lavender sphere) coalescing into the remnant horizon. The gravitons (purple particles) outside the larger surface are ejected as GW packets. The remaining gravitons would be trapped within the merging object, suggesting gravitons are confined in the remnant mass after coalescence.

4.3. Graviton Gas After Coalescence

This discussion is more of a thought experiment. Based on the previous discussion in Section 4.2.3 and the imagery provided in Figure 3, suppose not all gravitons are ejected at coalescence as the radiated GW. After the chirp phase, the binary collapses into a remnant mass; for a case of BBH and a BH-NS binary, the remaining gravitons would therefore be trapped inside a remnant black hole horizon. The thought experiment of so-called black hole gravitons is proposed in Ref. [26], under the conditions of virtual, i.e., spinless gravitons and given a Kerr black hole. However, the graviton gas mentioned throughout this report contains spin-2 gravitons, and this gas is

within an extremely rotating and contracting surface akin to an extreme Kerr outer surface.

In addition, the entropic energy at the chirp phase $|\Theta_{\text{chirp}}|$ would have to “cool” into the proper Hawking thermal energy for a Kerr black hole with the remnant mass m_f (c.f. Ref. [27]):

$$k_B T_H = \frac{\hbar \sqrt{m_f^2 - a^2}}{4\pi G m_f \left(m_f + \sqrt{m_f^2 - a^2} \right)}, \quad (28)$$

where $a \equiv J/m_f$ is a Kerr metric spin parameter with J being the total angular momentum. For a non-rotating black hole with $a = 0$, we recover the standard Hawking thermal energy $k_B T_H = \hbar/(8\pi G m_f)$. Assuming that the thermal equilibrium in the system-background ensemble is maintained after GW emission, there would be an ideal exponential decay law such that the cooling sequence $|\Theta_{\text{chirp}}| \rightarrow k_B T_H$ would take place. This cool-down is analogous to the ringdown phase, where the binary totally collapses and the metric perturbations level out into the canonical metric.

Should the black hole graviton thought experiment offered in Ref. [26] and in this discussion hold merit, this sets a hypothesis that black holes, either remnants of coalescence or otherwise ideal, harbor gravitons – a hypothesis that requires extensive mathematical foundation. This also speculates an alternative composition of Hawking radiation from rotating black holes as gravitonic; the power emitted from rotating black holes increases by a factor of up to 26 380 for gravitons [28], compared to the 1.9% graviton contribution to the emission power $P \propto \hbar/(G^2 M^2)$ from non-rotating black holes⁴ [29].

5. Conclusion

LIGO-based gravitational wave analysis demonstrates in numerous detections that the energy emitted at the chirp phase is scaled roughly by a tenth of the source chirp mass. Before this study, there lacks an analytical expression to accompany what numerical relativity calculates. As proposed in Section 1 and constructed in Section 2, relativistic kinetic theory is applied to GW astrophysics. In this heuristic approach, a characteristically extreme Kerr

⁴Provided the black hole mass is $M \gg 10^{14}$ kg; otherwise, for black hole mass 5×10^{11} kg $\ll M \ll 10^{14}$ kg, the graviton contribution to the emitted power is 1%.

outer surface traced by the coalescing binary contains an ultra-relativistic graviton gas with an effective thermal energy. Assuming there is thermal equilibrium between the system and the background, the energy contained in the coalescing binary is the energy emitted as background GWs. The brevity of Section 3 offers the derivation of the chirp phase entropic energy as Eq. (15), which analytically expresses the roughly one-tenth scaling of the chirp mass as emitted GW energy. Calculated values of analytical energy agree well with what was detected, provided select detections across all four observation runs of LIGO-VIRGO-KAGRA.

Correspondence between GWs and gravitons, which enabled the derivation of Eq. (15), opened branching topics of discussion that merits individual study. Of these discussion topics, the application of the Einstein-Langevin equation to Brownian noise analysis encourages the simulation of noise signals from the graviton gas within a specific volume $V \propto r(t)^3$. Additionally, the wave-particle duality between emitted GWs and monochromatic gravitons, and the characteristics of the graviton gas during and after coalescence (i.e., before and during the final ringdown phase) were also discussed. For a graviton gas during coalescence, a high energy graviton-graviton cross section was calculated to be roughly 1% of the chirp phase surface area $A = 16\pi G^2 \mathcal{M}^2$. The lattermost discussion humors the thought experiment of black holes harboring gravitons, as the logical consequence of the graviton gas after coalescence is its entrapment within the remnant black hole horizon. This supposes that, as a result, gravitons have a contribution to the composition to Hawking radiation, which was previously addressed by Don Page [28, 29].

Appendix A. Determining $r(t)$ for the Contracting Volume

In Section 2.1, a framework is established whereby a coalescing binary is contained in a contracting volume with radius $r(t)$. The conditions are set so that the diameter $d(t < t_C) = 2r(t < t_C)$ encloses the two masses and their separation distance (as seen in Figure 1), and that $r(t_C) = 2GM$. To ensure that the binary is perfectly encased, the diameter $d(t)$ is constructed as

$$d(t) = s(t) + r_1 + r_2 + s_{\text{correction}}, \quad (\text{A.1})$$

where $s(t)$ is the separation distance between two masses with radii r_1 , r_2 , and $s_{\text{correction}}$ is a “separation correction,” essentially a surplus factor to help ensure an enclosure of the whole binary.

In the case of coalescence, i.e., $r(t = t_C) = 2G\mathcal{M}$, we have via Eq. (A.1)

$$2G\mathcal{M} = \frac{1}{2} (s(t_C) + r_1 + r_2 + s_{\text{correction}}). \quad (\text{A.2})$$

Supposing that $s(t_C) = r_1 + r_2$, to suggest that inspiral ends (i.e., coalescence begins) when the two objects touch, the surplus factor $s_{\text{correction}}$ is defined as

$$s_{\text{correction}} = 4G\mathcal{M} - 2r_1 - 2r_2. \quad (\text{A.3})$$

Therefore, the diameter of the contracting volume that contains a coalescing binary is

$$d(t) = s(t) - r_1 - r_2 + 4G\mathcal{M}. \quad (\text{A.4})$$

The radii of the objects influence the calculation of the contracting radius $r(t) = d(t)/2$, ensuring a dependence on binary type (such as BBH, BNS, or BH-NS). Alongside half of the “vacuum separation” distance, the chirp mass Schwarzschild radius is the additive factor that helps enclose any coalescing binary within the contracting surface.

Appendix B. Alternative Derivations of Radiated GW Energy

In this appendix, two alternative derivations of the analytical radiated energy (in the report presented as Eq. [15]) are shown via the rotating body energy density (Eq. [2]) alone, and purely based on RK-Theory without considering the coalescing model constructed in Section 2.1.

Appendix B.1. GW Energy via Rotating Body T_{00}

In Section 2.1, the energy density of a rotating body via the EFEs is provided as a negative quantity. Therefore, extracting the energy by scaling away the spherical volume determines an expression for dissipative energy, i.e., radiating GWs. Therefore, Eq. (2) becomes

$$T_{00}V \equiv E(t) = -\frac{GM_{\text{encl}}(t)^2}{6r(t)} \left(1 + \frac{\beta(t)^2}{4}\right). \quad (\text{B.1})$$

At the chirp phase of coalescence, $M_{\text{encl}}(t_C) = \mathcal{M}$, $r(t_C) = 2G\mathcal{M}$ and $\beta(t_C) = 1$. Under these conditions, the dissipated energy at the chirp phase is

$$E(t_C) = \frac{-5}{48}\mathcal{M} \simeq -0.10417\mathcal{M}. \quad (\text{B.2})$$

While this derivation retrieves a nearly one-tenth scaling of the chirp mass (and it goes away from the relativistic kinetic theory of gravitons), the 1:1 ratios between Eq. (B.2) and detected values of energy, provided below in Table B.2, range from 0.8988 for the first set of values for GW190521 to 0.9900 for both GW150914 and the third set of values for GW190521. This range of ratios is wider than the 1:1 ratios between detected energies and Eq. (15), supposing that RK-Theory “fine-tunes” the analytical calculations.

GW Name	\mathcal{M}	E_{GW} (SI Units)	$ E(t_c) $ (SI Units)	1:1 Ratio
GW150914	$28.1^{+3.9}_{-3.5}M_{\odot}$	$3.0^{+0.5}_{-0.5}M_{\odot}c^2$	$2.97M_{\odot}c^2$	0.9900
GW151226	$8.9^{+0.3}_{-0.3}M_{\odot}$	$1.0^{+0.1}_{-0.2}M_{\odot}c^2$	$0.93M_{\odot}c^2$	0.9300
GW170104	$21.1^{+2.4}_{-2.7}M_{\odot}$	$2.0^{+0.6}_{-0.7}M_{\odot}c^2$	$2.17M_{\odot}c^2$	0.9217
GW170608	$7.9^{+0.2}_{-0.2}M_{\odot}$	$0.85^{+0.07}_{-0.17}M_{\odot}c^2$	$0.82M_{\odot}c^2$	0.9647
GW170814	$24.1^{+1.4}_{-1.4}M_{\odot}$	$2.7^{+0.4}_{-0.3}M_{\odot}c^2$	$2.51M_{\odot}c^2$	0.9296
GW190521	$64.0^{+13}_{-8}M_{\odot}$	$8.0M_{\odot}c^2$	$7.19M_{\odot}c^2$	0.8988
	$65.0^{+11}_{-7}M_{\odot}$	$7.0M_{\odot}c^2$	$7.19M_{\odot}c^2$	0.9736
	$71.0^{+15}_{-10}M_{\odot}$	$8.0M_{\odot}c^2$	$7.92M_{\odot}c^2$	0.9900

Table B.2: As like Table 1, emitted energies and associated chirp masses of select GWs detected by LIGO. The purely classical dissipated energies at the chirp phase (Eq. [B.2]) are calculated for each corresponding chirp mass for comparison with E_{GW} with 1:1 ratios.

Appendix B.2. GW Energy via RK-Theory

In statistical mechanics, the energy density can be conveniently defined as the coupling of the statistical number density and the average energy: $\epsilon = n\langle E \rangle$. However, instead of explicitly utilizing the Bose-Einstein distribution to evaluate $\langle E \rangle$, the semi-classical, macroscopic scale of the coalescing binary is taken advantage of by defining the expected energy enclosed as equivalent to the enclosed mass: $\langle E \rangle_{\text{encl}} = M_{\text{encl}}(t)$. Scaling away the volume of the

enclosure V from the energy density, we have the enclosed total energy:

$$\epsilon V \equiv E_{\text{tot, encl}} = N_{\text{encl}} M_{\text{encl}}(t). \quad (\text{B.3})$$

N_{encl} is the enclosed number of particles in a microstate. As it relates to massless BE-distributed gravitons with microstatic energy $\hbar\omega$, N_{encl} takes on the form of the Planck distribution, however not averaged by the graviton spin:

$$N_{\text{encl}} = \frac{2}{\exp(\hbar\omega/\Theta) - 1}. \quad (\text{B.4})$$

Recall that Θ was the quantity to obtain in this report. In this alternative derivation, Θ is irrelevant as long as the microstatic energy $\hbar\omega$ once again utilizes the thermal de Broglie wavelength. With $\hbar\omega \propto \Theta$, the microstatic number is a constant value: $N_{\text{encl}} = 2/(\exp(2\pi^{1/3}) - 1) = 0.11292$. Therefore, the enclosed total energy is roughly one-tenth of the enclosed rest energy:

$$E_{\text{tot, encl}} = 0.11292 M_{\text{encl}}(t). \quad (\text{B.5})$$

Straight-forwardly at the chirp phase, $M_{\text{encl}}(t_C) = \mathcal{M}$, and the discrepancy between the magnitude of Eq. (15) and Eq. (B.5) is negligible with a 1:1 ratio of 0.99965.

The above derivation goes away from the contracting geometry of the coalescing binary by simply scaling away the volume V . However, recall that the prefactor of Eq. (15) was obtained from the Kerr-like geometry of the binary at coalescence. The prefactor in Eq. (B.5) is set for all phases of coalescence, which makes no physical sense. The energy of intermediate GWs throughout coalescence is not one-tenth of the total mass, if the largest energy emission throughout GW formation is roughly one-tenth of the chirp mass. In other words, Eq. (B.5) is only valid for the chirp phase.

In both subsections, while it is possible to use one direction to obtain an expression of radiated energy, it is the symbiotic notion of quantum-classical correspondence that not only fine-tunes the calculations, but also implies contextual insight of the coalescing binary undergoing GW formation.

Appendix C. Deriving $\langle \hat{s} \rangle$ under BE Statistics

In Feynman diagram calculations, the \hat{s} -Mandelstam variable is defined as the square of the sum between the two incoming (or alternatively outgoing) 4-momenta of the external particle lines: $\hat{s} = (p_1 + p_2)^2 = (p_3 + p_4)^2$.

Conveniently, it is Lorentz-invariant; in the gas rest frame, the \hat{s} -Mandelstam variable is expanded and specifically defined for massless particles:

$$\hat{s} = p_1^2 + p_2^2 + 2p_1 \cdot p_2 = 2(E_1 E_2 - \vec{p}_1 \cdot \vec{p}_2). \quad (\text{C.1})$$

In the above, $p_i^2 = m_i^2$ via the 4-momentum product, which is equal to zero for massless particles. This leads to $E_i = |\vec{p}_i|$. In the gas rest frame, the 3-momenta are projected by their respective azimuthal and polar angles, where the dot product is taken in spherical coordinates:

$$\vec{p}_1 \cdot \vec{p}_2 = |\vec{p}_1| |\vec{p}_2| (\cos(\phi_1 - \phi_2) \sin \theta_1 \sin \theta_2 + \cos \theta_1 \cos \theta_2). \quad (\text{C.2})$$

This defines the \hat{s} -Mandelstam variable for massless particles in the gas rest frame as

$$\hat{s} = 2|\vec{p}_1| |\vec{p}_2| (1 - \cos(\phi_1 - \phi_2) \sin \theta_1 \sin \theta_2 - \cos \theta_1 \cos \theta_2). \quad (\text{C.3})$$

The thermal average of any quantity, such as \hat{s} , is defined as a two-distribution average:

$$\langle \hat{s} \rangle = \frac{1}{Z_1 Z_2} \iint_{-\infty}^{\infty} d^3 \vec{p}_1 d^3 \vec{p}_2 \hat{s} f_1(\vec{p}_1) f_2(\vec{p}_2). \quad (\text{C.4})$$

In general, this applies for any combination of two distribution functions, depending on the type of particles that are involved in the calculation of the quantity \hat{s} . For two massless bosons, such as gravitons, both distribution functions are the massless Bose-Einstein distribution, defined as Eq. (4). Thus, $Z_1 Z_2 = (Z_0)^2$, where $Z_0 = 8\pi\zeta(3)\Theta^3$ via Eq. (6).

The distribution functions, themselves, are only momentum-dependent, with no angular dependency. Via Eq. (C.3) and defining $d^3 \vec{p}_i = |\vec{p}_i|^2 d|\vec{p}_i| \sin \theta_i d\theta_i d\phi_i$, the 2-integral can be separated between the momentum part and the angular part:

$$\begin{aligned} \langle \hat{s} \rangle &= \frac{2}{(8\pi\zeta(3)\Theta^3)^2} I_{\text{mom.}} I_{\text{ang.}}, \\ \text{where } I_{\text{mom.}} &= \iint_0^{\infty} d|\vec{p}_1| d|\vec{p}_2| |\vec{p}_1|^3 |\vec{p}_2|^3 f_1(\vec{p}_1) f_2(\vec{p}_2) = \frac{\pi^8}{225} \Theta^8 \\ \text{and } I_{\text{ang.}} &= \iint_0^{\pi} d\theta_1 d\theta_2 \iint_0^{2\pi} d\phi_1 d\phi_2 \sin \theta_1 \sin \theta_2 \\ &\quad \times (1 - \cos(\phi_1 - \phi_2) \sin \theta_1 \sin \theta_2 - \cos \theta_1 \cos \theta_2) = 16\pi^2. \end{aligned} \quad (\text{C.5})$$

Therefore, the thermal average of the \hat{s} -Mandelstam variable under BE statistics is

$$\langle \hat{s} \rangle = \frac{\pi^8}{450\zeta(3)^2} \Theta^2 = 14.5927 \Theta^2. \quad (\text{C.6})$$

References

- [1] B. P. Abbott *et al.* [LIGO Scientific and Virgo], *Observation of Gravitational Waves from a Binary Black Hole Merger*, *Phys. Rev. Lett.* **116**, no.6 (2016) 061102 doi:10.1103/PhysRevLett.116.061102 [arXiv:1602.03837 [gr-qc]].
- [2] B. P. Abbott *et al.* [LIGO Scientific and Virgo], *GW151226: Observation of Gravitational Waves from a 22-Solar-Mass Binary Black Hole Coalescence*, *Phys. Rev. Lett.* **116**, no.24 (2016) 241103 doi:10.1103/PhysRevLett.116.241103 [arXiv:1606.04855 [gr-qc]].
- [3] B. P. Abbott *et al.* [LIGO Scientific and VIRGO], *GW170104: Observation of a 50-Solar-Mass Binary Black Hole Coalescence at Redshift 0.2*, *Phys. Rev. Lett.* **118**, no.22 (2017) 221101 [erratum: *Phys. Rev. Lett.* **121**, no.12 (2018) 129901] doi:10.1103/PhysRevLett.118.221101 [arXiv:1706.01812 [gr-qc]].
- [4] B. P. Abbott *et al.* [LIGO Scientific and Virgo], *GW170814: A Three-Detector Observation of Gravitational Waves from a Binary Black Hole Coalescence*, *Phys. Rev. Lett.* **119**, no.14 (2017) 141101 doi:10.1103/PhysRevLett.119.141101 [arXiv:1709.09660 [gr-qc]].
- [5] B. P. Abbott *et al.* [LIGO Scientific and Virgo], *GW170608: Observation of a 19-solar-mass Binary Black Hole Coalescence*, *Astrophys. J. Lett.* **851**, (2017) L35 doi:10.3847/2041-8213/aa9f0c [arXiv:1711.05578 [astro-ph.HE]].
- [6] R. Abbott *et al.* [LIGO Scientific and Virgo], *GW190521: A Binary Black Hole Merger with a Total Mass of $150M_{\odot}$* , *Phys. Rev. Lett.* **125**, no.10 (2020) 101102 doi:10.1103/PhysRevLett.125.101102 [arXiv:2009.01075 [gr-qc]].
- [7] R. Abbott *et al.* [LIGO Scientific and Virgo], *Properties and Astrophysical Implications of the $150 M_{\odot}$ Binary Black Hole Merger GW190521*,

- Astrophys. J. Lett.* **900**, no.1 (2020) L13 doi:10.3847/2041-8213/aba493 [arXiv:2009.01190 [astro-ph.HE]].
- [8] M. Parikh, F. Wilczek and G. Zahariade, *The Noise of Gravitons*, *Int. J. Mod. Phys. D* **29**, no.14 (2020) 2042001 doi:10.1142/S0218271820420018 [arXiv:2005.07211 [hep-th]].
- [9] M. Parikh, F. Wilczek and G. Zahariade, *Quantum Mechanics of Gravitational Waves*, *Phys. Rev. Lett.* **127**, no.8 (2021) 081602 doi:10.1103/PhysRevLett.127.081602 [arXiv:2010.08205 [hep-th]].
- [10] M. Parikh, F. Wilczek and G. Zahariade, *Signatures of the quantization of gravity at gravitational wave detectors*, *Phys. Rev. D* **104**, no.4 (2021) 046021 doi:10.1103/PhysRevD.104.046021 [arXiv:2010.08208 [hep-th]].
- [11] H. T. Cho and B. L. Hu, *Quantum noise of gravitons and stochastic force on geodesic separation*, *Phys. Rev. D* **105**, no.8 (2022) 086004 doi:10.1103/PhysRevD.105.086004 [arXiv:2112.08174 [gr-qc]].
- [12] B. S. DeWitt, *Quantum Theory of Gravity. 3. Applications of the Covariant Theory*, *Phys. Rev.* **162** (1967) 1239 doi:10.1103/PhysRev.162.1239
- [13] S. Rafie-Zinedine, *Simplifying Quantum Gravity Calculations* [arXiv:1808.06086 [hep-th]].
- [14] D. Blas, J. Martin Camalich and J. A. Oller, *Scalar resonance in graviton-graviton scattering at high-energies: The graviball*, *Phys. Lett. B* **827** (2022) 136991 doi:10.1016/j.physletb.2022.136991 [arXiv:2009.07817 [hep-th]].
- [15] R. L. Delgado, A. Dobado and D. Espriu, *Unitarized one-loop graviton-graviton scattering*, *EPJ Web Conf.* **274** (2022) 08010 doi:10.1051/epjconf/202227408010 [arXiv:2211.10406 [hep-th]].
- [16] M. Herrero-Valea, A. S. Koshelev and A. Tokareva, *UV graviton scattering and positivity bounds from IR dispersion relations*, *Phys. Rev. D* **106**, no.10 (2022) 105002 doi:10.1103/PhysRevD.106.105002 [arXiv:2205.13332 [hep-th]].

- [17] S. G. Fedosin. *Fizika i filozofia podobnii ot preonov do metagalaktik* (in Russian, Perm, 1999). ISBN 5-8131-0012-1.
- [18] S. R. de Groot, W. A. van Leeuwen, C. G. van Weert. *Relativistic Kinetic Theory: Principles and Applications* (Amsterdam, 1980).
- [19] B. L. Hu and A. Matacz, *Back reaction in semiclassical cosmology: The Einstein-Langevin equation*, *Phys. Rev. D* **51** (1995) 1577 doi:10.1103/PhysRevD.51.1577 [arXiv:gr-qc/9403043 [gr-qc]].
- [20] N. G. van Kampen. *Stochastic Processes in Physics and Chemistry* (Elsevier, Amsterdam, 1992).
- [21] N. M. MacKay, *Non-Equilibrium Noise in V-Shape Linear Well Profiles* doi:10.48550/arXiv.2406.16117 [arXiv:2406.16117 [cond-mat.stat-mech]].
- [22] D. Griffiths. *Introduction to Elementary Particle Physics* (John Wiley & Sons, Weinheim, 1987).
- [23] C. Rovelli and L. Smolin, *Knot Theory and Quantum Gravity*, *Phys. Rev. Lett.* **61** (1988) 1155 doi:10.1103/PhysRevLett.61.1155
- [24] C. Rovelli and L. Smolin, *Loop Space Representation of Quantum General Relativity*, *Nucl. Phys. B* **331** (1990) 80 doi:10.1016/0550-3213(90)90019-A
- [25] C. Rovelli and L. Smolin, *Discreteness of area and volume in quantum gravity*, *Nucl. Phys. B* **442** (1995) 593 [erratum: *Nucl. Phys. B* **456** (1995) 753] doi:10.1016/0550-3213(95)00150-Q [arXiv:gr-qc/9411005 [gr-qc]].
- [26] Y. Kimura, *Black hole graviton and quantum gravity*, *Phys. Scripta* **99**, no.4 (2024) 045024 doi:10.1088/1402-4896/ad338a [arXiv:2310.01925 [hep-th]].
- [27] K. Murata and J. Soda, *Hawking radiation from rotating black holes and gravitational anomalies*, *Phys. Rev. D* **74** (2006) 044018 doi:10.1103/PhysRevD.74.044018 [arXiv:hep-th/0606069 [hep-th]].

- [28] D. N. Page, *Particle Emission Rates from a Black Hole. 2. Massless Particles from a Rotating Hole*, *Phys. Rev. D* **14** (1976) 3260 doi:10.1103/PhysRevD.14.3260
- [29] D. N. Page, *Particle Emission Rates from a Black Hole: Massless Particles from an Uncharged, Nonrotating Hole*, *Phys. Rev. D* **13** (1976) 198 doi:10.1103/PhysRevD.13.198